MATHEMATICAL MODELING OF FLEXURAL DISK TRANSDUCERS FOR ARRAYS

E. M. Cliffel, Jr., et al

Hydroacoustics, Incorporated

Prepared for:

Naval Ships System Command

28 September 1973

Report No. HA 121-73

MATHEMATICAL MODELING OF FLEXURAL DISK TRANSDUCERS FOR ARRAYS

Contract NOOO24-72-C-1295

September 1973

HYDROACOUSTICS INC.

Report No. HA 121-73

MATHEMATICAL MODELING OF FLEXURAL DISK TRANSDUCERS FOR ARRAYS

E.M. Cliffel, Jr.

R.F. DeLaCroix

28 September 1973

Approved By: _____
R. L. Selsam
Director of Engineering

Approved By: _____
J. V. Bouyoucos
President

Submitted To:

Naval Ships System Command
Washington, D.C. 20360

Attention: Code PMS 302 - 42

Under Contract N00024-72-C-1295

HYDROACOUSTICS INC.

321 NORTHLAND AVE. P.O. BOX 3818 ROCHESTER, N. Y. 14610

(716) 544-2350

id

TABLE OF CONTENTS

LIST OF TABLES

LIST OF FIGURES

1.0 INTRODUCTION

A computer procedure(1)* was developed in 1971 for mathematical modeling the sinusoidal steady state dynamic behavior of composite flexural disks with radial symmetry in both construction and loading. This procedure computes the deflection profile for the composite disk and includes factors such as the finite restraint of achievable hinge edge support and the attachment to a finite backmass.

The program was first verified by predicting the behavior of several metal and piezoelectric bilaminar and trilaminar flexural disk assemblies which had been built under an earlier hardware development contract(2). Prediction accuracy of 1 to 3 percent in the resonant and antiresonant frequencies and 2 to 5 percent in the coupling factor was achieved. The modeling procedure was subsequently used in parametric studies of the effects of ceramic to metal backing thickness ratio, type of backing material and hinge clamping.

The modeling procedure consisted of 3 computer programs: "FLEX", which performed static deflection; "BOUCO", which applied general boundary conditions, including coupling of disk and hinge assemblies; and "DYANA", which computed the dynamic response of composite assemblies.

Under the current contract the DYANA program was retained but the functions of the two programs FLEX, and BOUCO were combined into a single program called HINGE-DISK. The capability of the HINGE-DISK program was then expanded to include the development of a stress matrix for computing the static or dynamic radial bending stresses in the composite disk or hinge. A stress matrix $[T]$ was developed in parallel with the flexibility matrix $[D]$ for the disk-hinge The $[T]$ matrix defined the radial stress

*Numbers in ( ) refer to references in Section 4.

at each point in the selected stress grid work as a function of the resultant contour loadings (F_n).

$$(T_i) = [T](F_n)$$

where (F_n) is the vector of total forces acting on the contours (accessible load ports)

and (T_i) is the vector of stresses evaluated at the selected points.

A separate report(3) was issued under this contract which provides a complete description of this expanded capability.

As part of this contract, the HINGE-DISK program was used to develop a multiport flexibility model for a typical bilaminar flexural disk transducer. The dynamic performance of a single transducer and a line array of three modules (each module is 2 transducers assembled back to back) was predicted using this multiport flexibility model as a basic building block. The computer program ARRAY was developed as a special hybrid version of the DYANA program to perform the dynamic array analysis.

Three different two port models were developed as approximations to the multiport model. The predicted dynamic performance of single two port modules, and line arrays of two ports, were compared against the full multiport model results which served as the standard of comparison.

The three two port models are designated as "in-air", "free field" and "array load" to distinguish between the load condition which was used in deriving their transfer admittance matrix parameters. These parameters for the "in-air" model are load independent whereas these parameters are load dependent in the other two models.

The computer modeling results show that large errors of up to 150% were obtained in the prediction of output volume velocity using the "in-air" two port. These errors were reduced by an order of magnitude by using the "free field" and "array load" two port models.

2.0 TWO PORT MODELS FOR A FLEXURAL DISK TRANSDUCER

The computer modeling procedure described in reference 1 yields a detailed model of a flexural disk transducer. It accurately portrays the axisymmetric behavior of a single transducer under a wide variety of load conditions by representing the disk as a series of interconnected rings, each of which is constrained to move uniformly at the average velocity of that portion of the disk it represents. This model is especially useful in studying the behavior of a single transducer or of small arrays of transducers such that the matrices required to describe the motion in detail do not exceed useful limits on computer storage and running time.

2.1 PURPOSE OF THE TWO PORT MODEL

The primary purpose of the two port model is to reduce the number of parameters required to compute the dynamic response of a single transducer from N^2 to 2^2, thereby allowing larger array problems to be handled efficiently. With proper care in defining the two port model, it is possible to maintain sufficient accuracy such that the reduced model can be used effectively in modeling arrays of transducers.

Two port models of flexural disk transducers have been used for some time. However, these models have been forced to use an assumed, or measured, deflection profile. A new modeling technique is described which defines the two port parameters using a detailed mathematical simulation of the dynamic behavior of the disk, its load and its attachments.

The "two port model" referred to throughout the text refers to the [b] matrix parameters as used in equation (1).

$$\begin{pmatrix} v \\ i \end{pmatrix} = \begin{bmatrix} b_{11} & b_{12} \\ b_{21} & b_{22} \end{bmatrix} \begin{pmatrix} f \\ \ell \end{pmatrix} \qquad (1)$$

Other forms of the model may be chosen as desired. For example, the ABCD matrix form can be obtained simply from the parameters of [b] as shown below:

$$\begin{pmatrix} e \\ i \end{pmatrix} = \begin{bmatrix} A & B \\ C & D \end{bmatrix} \begin{pmatrix} f \\ v \end{pmatrix}$$

where $A = -b_{11} / b_{12}$

$B = 1 / b_{12}$

$C = b_{21} - b_{11} \; b_{22}/b_{12}$

$D = b_{22}/b_{12}$

2.2 GENERAL CONSIDERATIONS IN THE DEVELOPMENT OF THE TWO PORT MODEL

The two port model is defined such that the input voltage and current, e and i, the average output velocity, v, and the output power of the reduced model are identical to that of the full N port model for two loading conditions. One such condition is that all models accurately predict the in air or unloaded multiport performance. Thus at any given frequency the parameters b_{12} and b_{22} are the same for all three procedures used to define the two port parameters. (See the table of parameters given in Appendix A.)

Sketches of the transducer and array models are given in Figure 1 and in more detail in Appendix B. The four rings closest to the center of the disk are defined as the radiating surfaces whereas the outermost ring including the hinge and housing are defined to be radiating into an infinite pressure release.

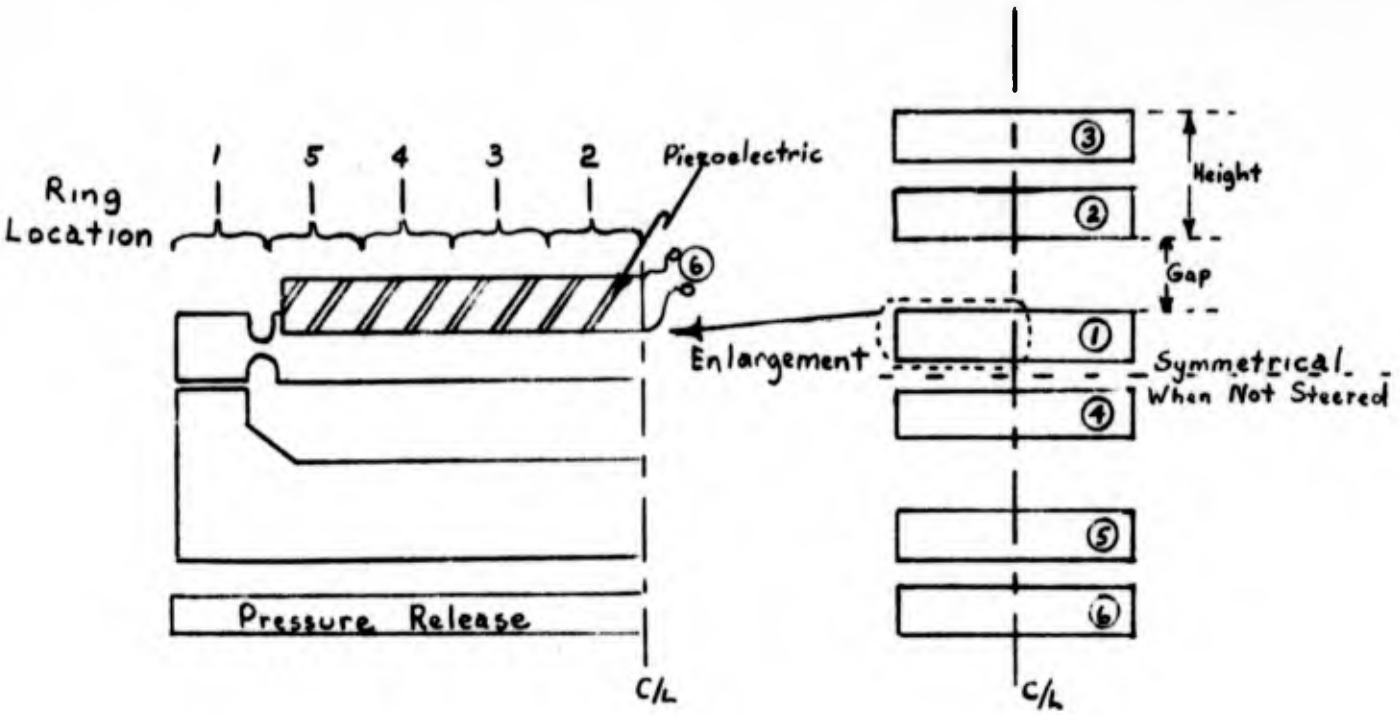

A Single Bilaminar Flexural Disk Transducer And A Line Array Of 3 Modules Assembled From 6 Transducers As Used In The Computer Modeling Study.

Figure 1.

The average velocity, $\bar{v}$, of the disk is defined by equation (2) as the total volume velocity from the radiating ports divided by the area of the disk.

$$\bar{v} = \left(\sum_{i=2}^{5} S(i)\, V(i) \right) / \mathcal{S} \qquad (2)$$

where

$S(i)$ = area of the ith ring segment

$\mathcal{S}$ = total area of the disk (i.e. the reference area)

The average external force, f, is defined to give the same output power for both the two port and the full N-Port models.

$$f = \frac{1}{N} \sum_{i=2}^{5} F^{*}(i) * V(i) \qquad (3)$$

where * denotes the complex conjugate

$F(i)$ - force on the ith ring from the multiport model

$V(i)$ - velocity of the ith ring from the multiport model

Equations (2) and (3) are used to define the two port parameters for two load conditions. The two port model defined by this procedure is then used to approximate the disk for other loads.

A different [b] matrix is computed at each frequency of interest. It is noted that even if the profile is independent of both frequency and loading, the parameters of the admittance matrix would show the following dependence on frequency:

$$b_{11} = j\omega \left(\frac{C_1}{1 - \omega^2 C_2} \right)$$

$$b_{12} = j\omega \left(\frac{C_1}{1 - \omega^2 C_2} \right) C_3$$

$$b_{22} = j\omega C_4 + j\omega \left(\frac{C_1}{1 - \omega^2 C_2} \right) C_3^2$$

where C_1, C_2, C_3, C_4 are constants (not required in further discussions of the model)

The radiation loading of the full multiport model was obtained by computing ring to ring $Z_{i,j}$'s using the computer program CHIEF. Each of the 6 radiating surfaces shown in Figure 1 is broken down into 5 segments of equal radial extent as shown in the detailed sketches at the end of Appendix B. The radiation loading for the two port model comes from combining the CHIEF ring to ring $Z_{i,j}$'s to maintain the power condition as defined by equation (3). The 6 X 6 matrix of impedance coefficients of the two port model, designated as $Z_{k,l}$'s could also have been obtained from other acoustic radiation programs for other geometrics. The underlying assumptions used in Appendix B to reduce the CHIEF $Z_{i,j}$'s to the two port $Z_{k,l}$'s are

a) the velocity distribution is known,
b) the velocity distribution is the same for all transducers, and
c) the velocity distribution is the same as used to define the two port parameters b_{11} and b_{21}.

The housing motion is computed explicitly in the multiport model but not in the two port model. The effect of housing motion however is approximated by deriving the two port parameters using the detailed single transducer model with a finite housing mass.

The housing of each transducer is assumed to be unloaded and decoupled from all other housings so that the two port model procedure can also be applied directly to the trivial case where the housing mass is infinite and hence not affected by loading. If the housings are coupled together, the two port procedure would not be sufficient and a three port procedure would be required. The three port procedure would extend the present two port procedure by retaining the housing explicitly.

2.3 THREE SPECIFIC TWO PORT MODELS

The three different two port models considered here ("in air", "free field", and "array load") may be distinguished as load dependent or load *in*dependent. The "in air" procedure is load independent and represents the general status of the flexural disk modeling prior to this contract. The [b] parameters derived by this procedure do not depend explicitly on a definition of load or force distribution; however, they can account for changes in the in air velocity profile with frequency.

The "free field" and "array load" procedures are termed load dependent since the numerical values of the parameters b_{11} and b_{21} depend on the choice of load distribution for which the reduced model can be compared exactly to the multiport model. For the "free field" model the load distribution is that on a single transducer operating in water without any baffles. For the "array load" model a priori knowledge of the array load distribution is assumed and this load is applied to a single transducer. In this analysis the two port parameters were derived using the loads acting on the center transducer of the array (for the smallest spacing between modules) as obtained from the full multiport analysis.

As indicated earlier the parameters b_{12} and b_{22} are the same for all three models at any one frequency because the two port model was defined to exactly match the multiport model for the condition of no load. The defining conditions for b_{12} and b_{21}, therefore, give rise to the condition that $b_{12} \neq b_{21}$ for the load dependent "free field" and "array load" procedures for computing the two port model parameters. The dependence of these parameters on load and frequency is given in functional form in Table 1.

Table 1.

Load and Frequency Dependence of the Two Port Parameters

Load Dependent

"In Air"		"Free Field"		"Array Load"
$b_{11}(\omega)$		$b_{11}(\omega, Z_1)$		$b_{11}(\omega, Z_2)$
$b_{21}(\omega)$		$b_{21}(\omega, Z_1)$		$b_{21}(\omega, Z_2)$
$b_{12} = b_{21}$		$b_{12} \neq b_{21}$		$b_{12} \neq b_{21}$
$b_{12}(\omega)$	=	$b_{12}(\omega)$	=	$b_{12}(\omega)$
$b_{22}(\omega)$	=	$b_{22}(\omega)$	=	$b_{22}(\omega)$

It is noted again that the two port model is precise only for the two conditions for which it was defined, and it gives an approximation elsewhere. Since there is an infinite choice of pairs of load conditions possible, it should be clear that the selection of the loading to define the "b" parameters is an arbitrary part of the procedure as defined in Appendix A. The actual loads experienced by a transducer in an array of fixed geometry vary over a considerable range depending on location in the array or the steering condition. The "free field" and "array load" procedures define models which represent a sampling from this range of loading conditions. For example, the loading of end transducers in a line array is nearly that of a transducer in a "free field" whereas those near the center of the array are more heavily loaded.

2.4 CALCULATION OF THE TWO PORT PARAMETERS

The calculation and use of the "b" parameters for a transducer involves use of a series of computer programs (1,3). The first step in the process is to compute the multiport flexibility model

of a single transducer using the program HINGE-DISK. The sinusoidal steady state deflections of the disk are then computed using the DYANA program with the flexibility model as one of its inputs. A second input to the dynamic analysis program is the specification of the electrical drive condition and the forces acting on the disk. The loads used to develop the "b" matrix parameters for the "free field" and "array load" two port models are obtained from the detailed model of a single transducer for the acoustic loading condition as defined by the matrix of impedance coefficients ($Z_{i,j}$'s). The two port parameters are computed as part of the ARRAY* program when the detailed analysis of a single transducer is performed with the loading prescribed. A separate program is used to take the $Z_{i,j}$'s for the multiport model and reduce them down to a smaller set of $Z_{k,l}$'s to be used in the two port modeling of an array.

In order to compare the two port model to the full multiport solution the program DYANA is used to compute the dynamic behavior of an array of electroacoustic transducers, each of which is defined by the same two port model. For the 6 transducer test array, the two port DYANA model was specified by a 12 by 12 flexibility matrix and the 6 by 6 $Z_{k,l}$ matrix defining the loading of the mechanical ports only. For convenience in using the DYANA program directly, the two port flexibility matrix rather than the two port admittance matrix was employed in the modeling study. The flexibility matrix of a single transducer is obtained by dividing the two port admittance matrix [b] by the factor $j\omega$.

A full multiport model for the 6 transducer array is computed using a special version of the DYANA program. This latter program has been modified to allow for the solution of the 36 by 36 model which results from considering a 6 by 6 flexibility model for each transducer. In general, this latter program designated ARRAY would not be required. It's purpose here was to develop a base performance prediction against which the two port models could be compared.

*Modified DYANA program

2.5 ARRAY PERFORMANCE PREDICTIONS

The mutual impedance terms in the array caused the magnitude of the effective transducer loading to vary over an approximate range of about 7 to 1, as is shown in Table 2. This range of loading provided a reasonable test of the utility of the two port model. The impedances for a single module in a free field given in Table 2 are used in defining the "free field" two port model. Note that the "free field" two port model is used to predict the array performance for loads with magnitude are as great as 3 times the load from which the b_{11} and b_{21} parameters are defined.

Table 3 provides a comparison of the accuracy achieved by the three different two port models in duplicating the predictions of the full multiport model. This table presents the relative error of each prediction in percent and degrees of phase difference with respect to the multiport performance parameters for 3 different frequencies and 2 different module spacings.

The data of *Table 3* clearly shows that the prediction errors of the "in air" procedure are in the range of 30 to 150%. The data also show that the two load dependent two port models give more accurate predictions than the "in air" model with the exception of the "array load" model at 1000 Hz and large gap. For the latter condition the "array load" two port model predictions and the "in air" model predictions are comparable.

Freq.	Surface	Module in a Free Field		Free Field Two Port Array Model			
				Gap = .200M		Gap = .050M	
(Hz)		R/ρcA	X/ρcA	R/ρcA	X/ρcA	R/ρcA	X/ρcA
550.	1	.0080	.300	Not Avail-	Not Avail-	.104	1.001
	2			able	able	.104	1.000
	3					.076	.371
700.	1	.0133	.393	.143	.585	.150	1.288
	2			.140	.581	.150	1.287
	3			.089	.439	.122	.461
850.	1	.0202	.495	.189	.709	.162	1.611
	2			.186	.705	.162	1.612
	3			.104	.516	-.845	-1.307
1000.	1	.0293	.611	.246	.803	.439	1.865
	2			.236	.807	.428	1.828
	3			.096	.670	.082	.681
1150.	1	.0413	.744	.291	.956	.417	2.265
	2			.281	.959	.417	2.265
	3			.114	.793	.119	.805
1300.	1	.0570	.901	.342	1.126	.480	2.721
	2			.331	1.133	.480	2.720
	3			.131	.952	.145	.958

$\rho cA = 1.261 * 10^5$ Kg/sec

Table 2 Specific Load Impedance Values For A Single Transducer In A Free Field And For A Line Array of 6 Transducers

Table 3 also shows that it is possible to improve the prediction accuracy of the two port model by selecting a more appropriate load distribution for defining the "b" parameters as was done in the "array load" procedure. The "array load" two port model prediction errors were less than 4% at 550 and 700 Hz. In general the "array load" model is an improvement over the "free field" model. However, at 1000 Hz the "array load" model appears to be less accurate than the "free field" procedure. The larger error of the "array load" procedure at 1000 Hz seems to be related to the accuracy of the value assigned to the two port impedances $Z_{k',1}$ rather than to the "b" parameters defining the model. This frequency is close to the 1054 Hz resonant frequency of the transducer where the source impedance of the transducer itself is approaching 0.0. For this condition the accuracy of the output velocity prediction will correspond to the accuracy to which the load is known.

Since the "free field" two port model offers increased accuracy over the "in air" procedure and does not require any estimates of the transducer loading in an array, it seems likely that this procedure may be used most often. A more complete comparison of the "free field" model predictions relative to the full multiport model are therefore compiled below.

Table 4 shows that the "free field" two port model gives good or acceptable results with nominal errors in the range of 3 to 10%. The exception to this rule is that above the in air resonant frequency of a single transducer, f_R = 1054.Hz, the errors are as large as 20% for the small gap array. In addition an extreme error of 45% was found for the end module prediction at 850 Hz. This latter case corresponds to a large negative real impedance as given in Table 2. Both the "free field" two port model and the full multiport model predict that the end module is delivering a negative amount of power to the acoustic field for this condition. The probability of errors of this magnitude should be minimized by designing arrays such that this undesirable feed back condition is avoided.

Freq. (Hz)	Variable	Gap = .200M Per Cent and Degrees Phase Difference Load Dependent			Gap = .050M Per Cent and Degrees Phase Difference Load Dependent		
		Free Field	Array Load	In Air	Free Field	Array Load	In Air
550.	$v(1)$	Not Computed	Not Computed	Not Computed	+14. ∠-1.	+0. ∠ 0.	+103. ∠-6.
	$v(2)$				+14. ∠-1.	+0. ∠ 0.	+103. ∠-6.
	$v(3)$				+ 3. ∠-1.	-4. ∠ 0.	+ 27. ∠-4.
	$i(1)$				- 0. ∠ 0.	0. ∠ 0.	+ 2. ∠+0.
	$i(2)$				- 0. ∠ 0.	0. ∠ 0.	+ 2. ∠+0.
	$i(3)$				0. ∠ 0.	-0. ∠ 0.	- 0. ∠ 0.
700.	$v(1)$	5. ∠-2.	-0. ∠-0.	+37. ∠-8.	+14. ∠-2.	+0. ∠-2.	+148. ∠-12.
	$v(2)$	5. ∠-2.	-0. ∠-0.	+36. ∠-8.	+14. ∠-2.	+0. ∠-2.	+148. ∠-12.
	$v(3)$	2. ∠-1.	-2. ∠ 0.	+21. ∠-5.	+ 3. ∠-1.	-2. ∠+3.	+ 23. ∠- 9.
	$i(1)$	-0. ∠ 0.	+0. ∠ 0.	+ 0. ∠-1.	- 0. ∠ 0.	-2. ∠+0.	+ 11. ∠- 3.
	$i(2)$	-0. ∠ 0.	+0. ∠ 0.	+ 0. ∠-1.	- 0. ∠ 0.	-2. ∠+0.	+ 11. ∠- 3.
	$i(3)$	-0. ∠ 0.	+1. ∠-0.	- 0. ∠-0.	- 0. ∠ 0.	+0. ∠+58.	- 0. ∠- 1.
1000.	$v(1)$	-10. ∠-2.	-33. ∠-4.	+26. ∠+11.	- 0. ∠-2.	-17. ∠-2.	+ 13. ∠+ 5.
	$v(2)$	-10. ∠-2.	-33. ∠-3.	+25. ∠+10.	+ 0. ∠-2.	-18. ∠-2.	+ 12. ∠+ 5.
	$v(3)$	-13. ∠-1.	-41. ∠+1.	+43. ∠+8.	-13. ∠-0.	-41. ∠+3.	+ 20. ∠+ 5.
	$i(1)$	+ 4. ∠-4.	- 9. ∠+28.	+96. ∠-4.	- 2. ∠-1.	- 0. ∠+0.	+ 26. ∠- 3.
	$i(2)$	+ 4. ∠-3.	- 7. ∠+28.	+92. ∠-4.	- 2. ∠-1.	+ 0. ∠+0.	+ 26. ∠- 3.
	$i(3)$	+ 4. ∠-1.	-51. ∠+49.	+131. ∠+4.	+ 5. ∠-0.	-50. ∠+58.	+ 61. ∠+10.

Table 3 Two Port Model Prediction Errors Relative To The Multiport Model At Three Different Frequencies And Two Different Gaps Between Modules

Per Cent and Degrees Phase Difference

Load Dependent "Free Field" Two Port Model

Gap	Variable	550.Hz	700.Hz	850.Hz	1000.Hz	1150.Hz	1300.Hz
.200M	$\nu(1)$	Not Run	+5. ∠-2.	+4. ∠-3.	-10. ∠-2.	+ 6. ∠-2.	+ 6. ∠-2.
	$\nu(2)$		+5. ∠-2.	+3. ∠-2.	-10. ∠-2.	+ 6. ∠-2.	+ 6. ∠-3.
	$\nu(3)$		+2. ∠-1.	+0. ∠-0.	-13. ∠-1.	+ 3. ∠-1.	+ 2. ∠-0.
	$i(1)$		-0. ∠ 0.	-1. ∠-0.	+ 4. ∠-4.	- 0. ∠-0.	+ 1. ∠-17.
	$i(2)$		-0. ∠ 0.	-0. ∠-0.	+ 4. ∠-3.	- 0. ∠-0.	+ 2. ∠-17.
	$i(3)$		-0. ∠-0.	-0. ∠+0.	+ 4. ∠-1.	- 0. ∠+0.	+ 2. ∠-15.
.050M	$\nu(1)$	+14. ∠-1.	+14. ∠-2.	+10. ∠+21.	-0. ∠-2.	+20. ∠-2.	+22. ∠-2.
	$\nu(2)$	+14. ∠-1.	+14. ∠-2.	+10. ∠+21.	+0. ∠-2.	+20. ∠-2.	+22. ∠-2.
	$\nu(3)$	+ 3. ∠-1.	+ 3. ∠-1.	-45* ∠-18.	-13. ∠-0.	+ 3. ∠-0.	+ 3. ∠-1.
	$i(1)$	- 0. ∠-0.	- 0. ∠-0.	- 0. ∠+23.	-2. ∠-1.	- 0. ∠ 0.	+ 5. ∠-20.
	$i(2)$	- 0. ∠ 0.	- 0. ∠ 0.	- 0. ∠+23.	-2. ∠-1.	- 0. ∠ 0.	+ 5. ∠-20.
	$i(3)$	0. ∠ 0.	- 0. ∠ 0.	-15* ∠-13.	+5. ∠-0.	- 0. ∠+0.	+ 2. ∠-15.

*Both The Multiport and Two Port Models Predict A Negative Resistive Load For This Transducer. It is absorbing power from the acoustic field.

Table 4. "Free-Field" Two Port Model Prediction Errors Relative To The Multiport Model At Six Frequencies and Two Different Gaps Between Modules.

3.0 CONCLUSIONS AND RECOMMENDATIONS

The two load dependent two port models which were developed offer a considerable improvement in prediction accuracy over the traditionally accepted "in air" two port model.

The "free field" procedure has a significant advantage over the "array load" procedure in so far as it is not difficult for the designer to understand the load conditions for which it was defined. The "free field" descriptor, therefore, implies a nominal load range for which the two port model predictions will be most accurate. In reviewing array performance predictions using this model it is then possible for the designer to apply a judgment factor as to how accurate the predictions might be depending on the actual individual transducer loads relative to the "free field" case.

For the "array load" two port model to be used to greatest advantage it would be best to categorize array elements according to their anticipated nominal loading and then to develop a set of [b] matrix parameters suitable for this loading. Thus more than one two port model would be required at any one frequency for predicting the array performance.

The two port models are all limited to cases where there is no direct connection between the housings of individual transducers. Thus the case of line arrays where individual transducers are mounted back to back in pairs cannot be handled in general. To remedy this problem it would be necessary to construct a three port model and use the additional port to describe the housing as a separate radiation port to which attachments (such as an additional transducer) could be made. It is, therefore, recommended that future work include the development of a three port model.

Since the "free field" procedure was not shown to be optimum, it would be of considerable interest to expand the present work to investigate potential avenues of further improvement. Generalization of the procedure to allow defining the two port model [b] matrix parameters using two actual load distributions should be pursued.

4.0 REFERENCES

1. Performance Prediction Model for Radially Symmetric Flexural Disk Transducer
   Cliffel, E. M., DeLaCroix, R. F.
   Report HL 101-72: Contract N00140-71-C-0081
   General Dynamics Electronic Division
   February 1972

2. Flexural Disk Transducer Development
   H. J. Straube
   Report No. AC 104-70: Contract N00140-69-C-0174
   General Dynamics Electronics Division
   May 1, 1970

3. Stress Computations In the General Flexural Disk Model
   Cliffel, E. M., DeLaCroix, R. F.
   Report No. 108-73: Contract N00024-72-C-1295
   April 1973

APPENDIX A DEVELOPMENT OF THE TWO PORT MODEL

The purpose of this development is to obtain a two port model which is an approximation to the multiport model for the axisymmetric vibration of a circular plate. The two port model is defined by equation (1) in terms of the average velocity of the radiating surface, v, f and e and the input current i.

$$\begin{pmatrix} v \\ i \end{pmatrix} = \begin{bmatrix} b_{11} & b_{12} \\ b_{21} & b_{22} \end{bmatrix} \begin{pmatrix} f \\ e \end{pmatrix} \qquad (1)$$

The two port model must be related to the full multiport model as defined by equation (2).

$$\begin{pmatrix} (V) \\ I \end{pmatrix} = \begin{bmatrix} [A_1] & (A_2) \\ (A_3) & A_{n,n} \end{bmatrix} \begin{pmatrix} (F) \\ E \end{pmatrix} \qquad (2)$$

where (V) - Multiport Vector of Ring Velocities

(F) - Multiport Vector of Ring Force

I, E - Electrical Drive Port Parameters of the Multiport Model

$[A]$ - Partitioned matrix - derived at the end of Appendix A

The task is to *define* the parameters of the two port model b_{11}, b_{12}, b_{21}, and b_{22}. Thus 4 independent equations are required in which the b parameters are the only unknowns. The necessary equations can be obtained from equation (1) if a set of relations are provided whereby the two port parameters v, i, f, and e can be treated as known functions of the multiport input and output variables. Equations (3) thru (7) describe the manner in which the two port model and the multiport model are defined.

$$e = E \tag{3}$$

$$i = I \tag{4}$$

$$v = \left[\sum_i (S(i)V(i)\right] / \mathcal{S} = (S)^T(V)/\mathcal{S} \tag{5}$$

$$f^* v = \sum_i F^*(i)V(i) = (F^*)^T(V) \tag{6}$$

$$\mathcal{S} = \sum_j S(j) \tag{7}$$

where

f^* is the complex conjugate of f.

$F^*(i)$ is the complex conjugate of $F(i)$.

$S(i)$ is the area of the ith ring.

The range of i is to include radiating ports from which the average velocity v is computed. The range of j can be chosen as desired since the parameter $\mathcal{S}$ is only a scaling factor.

Equations (3) thru (7) define the two port input and output parameters for any choice of the general load vector (F) and velocity distribution (V) of the multiport model.

The four equations required to define the "b" parameters are then obtained by writing equation (1) for two different driving conditions $\begin{pmatrix} F_1 \\ E_1 \end{pmatrix}$ and $\begin{pmatrix} F_2 \\ E_2 \end{pmatrix}$, for which the two port equivalent drive conditions are $\begin{pmatrix} f_1 \\ e_1 \end{pmatrix}$ and $\begin{pmatrix} f_2 \\ e_2 \end{pmatrix}$ respectively.

The computed values of the "b" parameters for the three models considered in this report are given in Table A.1.

$b_{21}/j\omega$ and $b_{11}/j\omega$ For Different Two Port Models

f	(units of 10^{-9}) $b_{22}/j\omega$ (Real)	$b_{12}/j\omega$ (Real)		"In Air" (Real)	(Imag)	Load Dependent "Free Field" (Real)	(Imag)	"Array Load" (Real)	(Imag)
550.	68.151	3.2350	$b_{21}/j\omega$	3.2350	0.0	3.0326	-.01304	2.7036	-.09623
			$b_{11}/j\omega$	.81148	0.0	-.64582	.02198	-.80805	.06248
700.	72.056	4.1743	$b_{21}/j\omega$	4.1743	0.0	3.8964	-.2236	3.4502	-.00144
			$b_{11}/j\omega$	1.03832	0.0	.10361	.01468	-.04987	.02582
850.	82.101	6.5930	$b_{21}/j\omega$	6.5930	0.0	6.1191	-.04560	N.A.	N.A.
			$b_{11}/j\omega$	N.A.	0.0	.92063	.00600	N.A.	N.A.
1000.	148.487	22.2587	$b_{21}/j\omega$	22.2587	0.0	20.8097	-.19918	18.2613	-1.8106
			$b_{11}/j\omega$	5.48841	0.0	4.62537	-.03298	3.9933	-.36928
1150.	5.485	-11.8718	$b_{21}/j\omega$	-11.8718	0.0	-10.8361	.13295	N.A.	N.A.
			$b_{11}/j\omega$	N.A.	0.0	-2.89423	.04576	N.A.	N.A.
1300.	37.179	-4.2382	$b_{21}/j\omega$	-4.2382	0.0	-3.8230	.06022	N.A.	N.A.
			$b_{11}/j\omega$	N.A.	0.0	-1.13282	.02738	N.A.	N.A.

units b_{11} (M/N.Sec), b_{12} (M/V.Sec), b_{21} (coulomb/N.Sec), b_{22} (coulomb/V.Sec)

Table A.1 Complex Two Port Parameter Values Derived by Three Different Modeling Procedures.

A.1 SELECTION OF THE LOAD DISTRIBUTION

The two force vectors (F) which are used to develop the two port model may be arbitrarily chosen. The degree to which the two port model will approximate the multiport model over a wide range of conditions will depend on the appropriateness of the original choice relative to actual array loads.

In the procedure which follows, the following choice was made:

1. $(F) = (0)$ The null force vector representing the in air operating case was used in all the models. Therefore, the two port model predicts the in air performance with the same accuracy as the multiport model.

2. $(F) = g(Z,V)$ The force distribution was defined from some real impedance loading, i.e. a single module in a free field or a single transducer as loaded in a particular array position.

A.2 PARAMETERS b_{12} and b_{22} DEFINED BY THE IN AIR LOAD DISTRIBUTION

The equivalent two port model load, f , is obtained from equation (6) which specifies that both the multiport and two port models will predict the same total power for the defining load distribution.

$$f^* = f = 0 \qquad ,(F) = (0)$$

From the two port and multiport models, equations (1) and (2), we obtain the following:

$$\begin{aligned} \sim &= b_{12} e \\ i &= b_{22} e \end{aligned} \qquad ; f = 0 \ , e \neq 0 \qquad (8)$$

$$\begin{aligned} V &= (A_{v,n}) E \\ I &= A_{i,n} E \end{aligned} \qquad ,(F) = (0) \ , E \neq 0 \qquad (9)$$

Combining the velocity equations from (8) and (9) with equations (3) and (5) yields

$$b_{12}\, e = b_{12} E = (S)^T (A_2) \epsilon / \mathcal{S} = \frac{(A_2)^T (S) E}{\mathcal{S}}$$

$$b_{12} = (A_2)^T (S) / \mathcal{S} \qquad (10)$$

Similarly the current equations from (8) and (9) may be combined with equations (3) and (4) to give

$$b_{22}\, e = b_{22} E = A_{n,n}\, E$$

$$b_{22} = A_{n,n} \qquad (11)$$

A.3 PARAMETERS b_{11} and b_{21} DEFINED BY A NON ZERO LOAD DISTRIBUTION

The equivalent two port load f is obtained from the power and velocity relations as given by equations (5) and (6)

$$f^* = \mathcal{S} \frac{(F^*)^T (V)}{(S)^T (V)} \quad , (F) \neq (0)$$

$$f^* = \mathcal{S} \frac{(F^*)^T \{[A_1](F) + (A_2) E\}}{(S)^T \{[A_1](F) + (A_2) E\}}$$

Since $\mathcal{S}$, $(S)^T$ and the general $[A]$ matrix are purely real the complex conjugate of f^* is given by equation (12).

$$f = \mathcal{S} \frac{(F)^T \{[A_1](F^*) + (A_2) E^*\}}{(S)^T \{[A_1](F^*) + (A_2) E^*\}} \qquad (12)$$

The parameter b_{11} can be defined by rearranging the velocity equation from (1).

$$b_{11} = (v - b_{12} e)/f$$

By substituting for v and e from equations (5) and (3) respectively we obtain:

$$b_{11} = \{(S)^T(V)/S - b_{12} E\}/f \qquad (13)$$

Proceeding in an analogous fashion we obtain an expression for b_{21} by rearranging the current equations from (1).

$$b_{21} = (i - b_{22} e)/f$$

By substituting for e and i from equations (3) and (4) respectively and using I as defined by equation (2) we obtain

$$b_{21} = (A_3)(F)/f \qquad (14)$$

The four parameters of the two port model are therefore defined by equations (10), (11), (13) and (14) along with equation (12) which is used to obtain the value of the equivalent load, f, required in (13) and (14).

We note that the admittance parameters b_{11} and b_{21} as defined by equations (13) and (14) depend explicitly on the load distribution acting on the disk (F). The procedure could be generalized to allow the two port model to be defined by two non zero load distributions (F) $\neq$ (O). In the latter case all 4 of the parameters b_{11}, b_{12}, b_{21}, b_{22} would depend explicitly on (F) and there would be some reduction in accuracy of the two port model predictions of the unloaded dynamic performance with respect to the procedures outlined above.

A.4 THE "IN AIR" MODEL PARAMETERS

The "in air" two port model has no load dependence and therefore the parameter b_{11} is computed from equation (15) rather than as derived in section A.3. The functional form $b_{11}(f)$ implies a dependence on frequency as in the load dependent model.

$$b_{11}(f) = \frac{(b_{21}(f))^2}{[b_{22}(f) - j\omega C_{Low}(f_R/f_A)^2]} \qquad (15)^*$$

where

C_{Low} = Low freqency capacitance

f_R = Resonance Frequency in Air

f_A = Antiresonance Frequency in Air

and $C_{Low} = D_{n,n}$ (From n x n disk flexibility matrix)

The parameters b_{12} and b_{22} are computed from equations (10) and (11) as before. However, the parameter b_{21} is now defined by equation (16)

$$b_{21} = b_{12} \qquad (16)$$

A.5 VECTOR *DIMENSIONS* OF THE ELECTROACOUSTIC SAMPLE PROBLEM

For the specific cases considered here, the loaded ports in the multiport problem are ports 2 through 5. Thus the summation range required in equations (5) and (6) is $i = 2,3,4,5$. The edge ring, port 1, is connected to the housing and is assumed to be

*"In Air" Two Port Model only

radiating into an ideal pressure release and hence is not included in these summations.

The reference area $\mathcal{S}$ is obtained by summing over the entire disk j = 1,2,3,4,5. This range was arbitrarily chosen since it gives the total area of the disk. We note again that this is only a scaling factor which the total volume velocity was divided by to obtain the average velocity $\mathcal{V}$. To obtain the total volume velocity predicted by the two port model, we must perform the multiplication $\mathcal{V} \cdot \mathcal{S}$. The two port model gives the volume velocity regardless of the choice of $\mathcal{S}$ (i.e. for $S \neq 0$)

A.6 THE "[A]" MATRIX REQUIRED FOR DEFINING TWO PORT MODEL PARAMETERS

The general multiport model is defined by the following equation

$$[A]\begin{pmatrix}(W)\\ g\end{pmatrix} = [D]\left\{\begin{pmatrix}(F)\\ E\end{pmatrix} + \omega^2[M]\begin{pmatrix}(W)\\ g\end{pmatrix}\right\}$$

This equation can be rearranged by taking the mass dependent terms over to the L. H. S. of the equation leaving all the applied forces and the load forces on the R.H.S.

$$\left[[A] - \omega^2[D][M]\right]\begin{pmatrix}(W)\\ g\end{pmatrix} = [D]\begin{pmatrix}(F)\\ E\end{pmatrix}$$

By simply grouping terms we can re-write the preceding equation in the following form:

$$\begin{pmatrix} (W) \\ g \end{pmatrix} = [\,G\,] \begin{pmatrix} (F) \\ E \end{pmatrix} \tag{17}$$

where $$[G] = \left[\,[A] - \omega^2 [D][M]\right]^{-1} [D] \tag{18}$$

Equation (17) can be expressed in terms of the sinusoidal steady state velocities as follows:

$$\begin{pmatrix} (V) \\ i \end{pmatrix} = [A] \begin{pmatrix} (F) \\ E \end{pmatrix} \tag{19}$$

where $$[A] = j\omega [G]$$

$$[A] = j\omega \left[[A] - \omega^2 [D][M]\right]^{-1} [D] \tag{20}$$

APPENDIX B DIMENSIONS AND SPECIFICATIONS OF THE ARRAY AND THE ARRAY LOADING

The basic transducer dimensions and its mechanical properties are given in Figure B.1, and Table B.1. Each transducer is broken down into 5 uniform size rings for the computation of the $Z_{i,j}$ radiation loads using the computer program CHIEF. The numbering of the elements for the $Z_{i,j}$ computation differs from that of the full dynamic model as shown in Figure B.2 because of the interleaving of the electrical ports.

The equivalent two port loading is obtained from the multiport $Z_{i,j}$'s by using the equivalent power condition as defined by equation (6) of Appendix A.

The power from the k^{th} disk is given by

$$f_k^* v_k = \sum_{i}^{\text{Ports of disk } k} F^*(i)\, V(i) \qquad (1)$$

The force F(i) can be further broken down to define the partial force on the k^{th} disk which results from the motion of the l^{th} disk as follows:

$$\left(\sum_{l}^{\text{all disks}} f_{k,l}^* \right) v_k = \sum_{j}^{\text{all ports}} \left\{ \sum_{i}^{\text{ports of disk } k} F^*_{i,j}\, V_i \right\} \qquad (2)$$

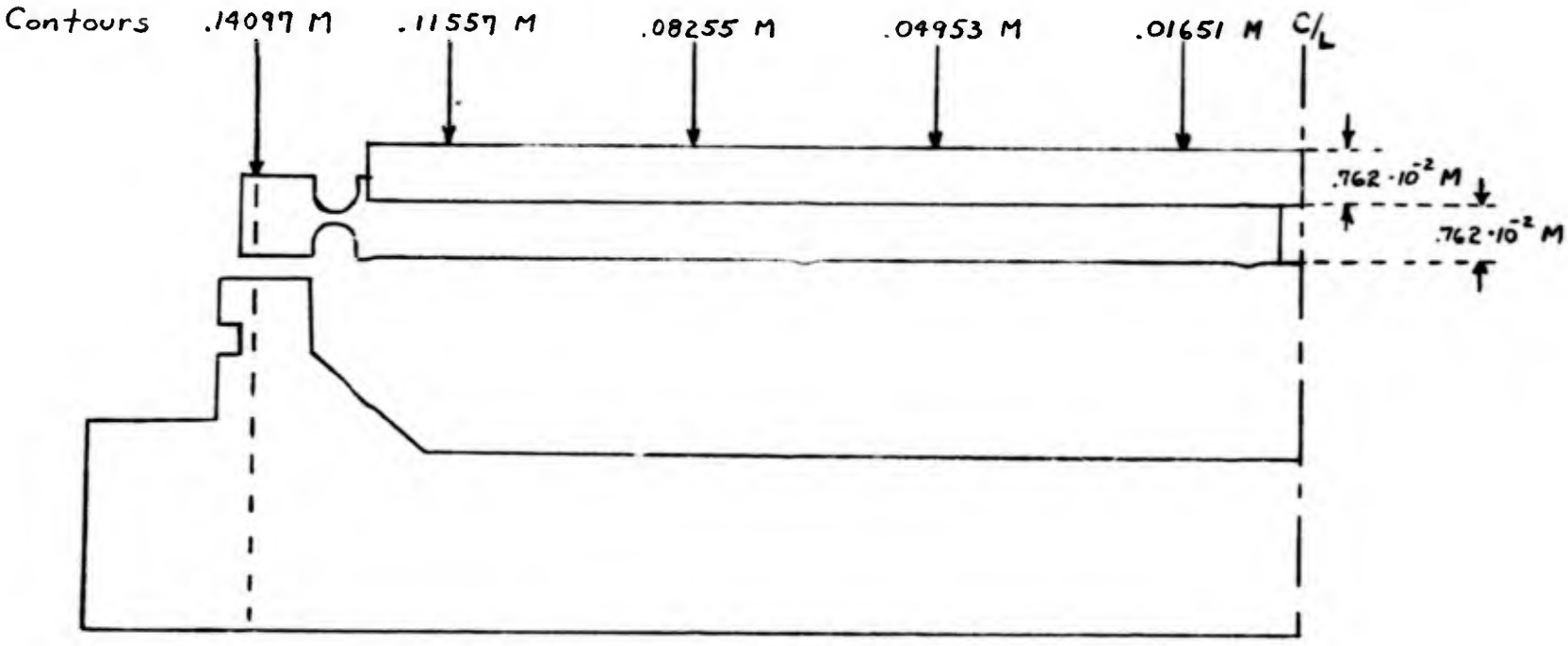

Figure B.1 Transducer Dimensions

Table B.1 Specifications-Electroacoustic Module

Material Properties

	Steel		Ceramic (Chan 5400)	
ρ (Kg/M^3)	7860.		7600.	
S^D_{11} (M^2/N)	4.83	E-12	1.050	E-11
S^E_{12} (M^2/N)	-1.60	E-12	-5.10	E-12
S^E_{33} (M^2/N)	1.286	E-11	1.93	E-11
g_{31} (V·M/N)	0.0		10.60	E-03
ε^T_{33} farad/M	0.0		11.51	E-09

Final 5 x 5 Flexibility Matrix
(MKS Values in units of 10^{-9})

	1	2	3	4	5
1	18.145	14.074	8.5795	2.7543	11.850
2	14.048	11.763	7.4077	2.4136	10.308
3	8.5447	7.3868	5.0699	1.7341	7.2300
4	2.7170	2.3835	1.7163	.71472	2.6150
5	11.302	10.365	7.2869	2.6671	64.621

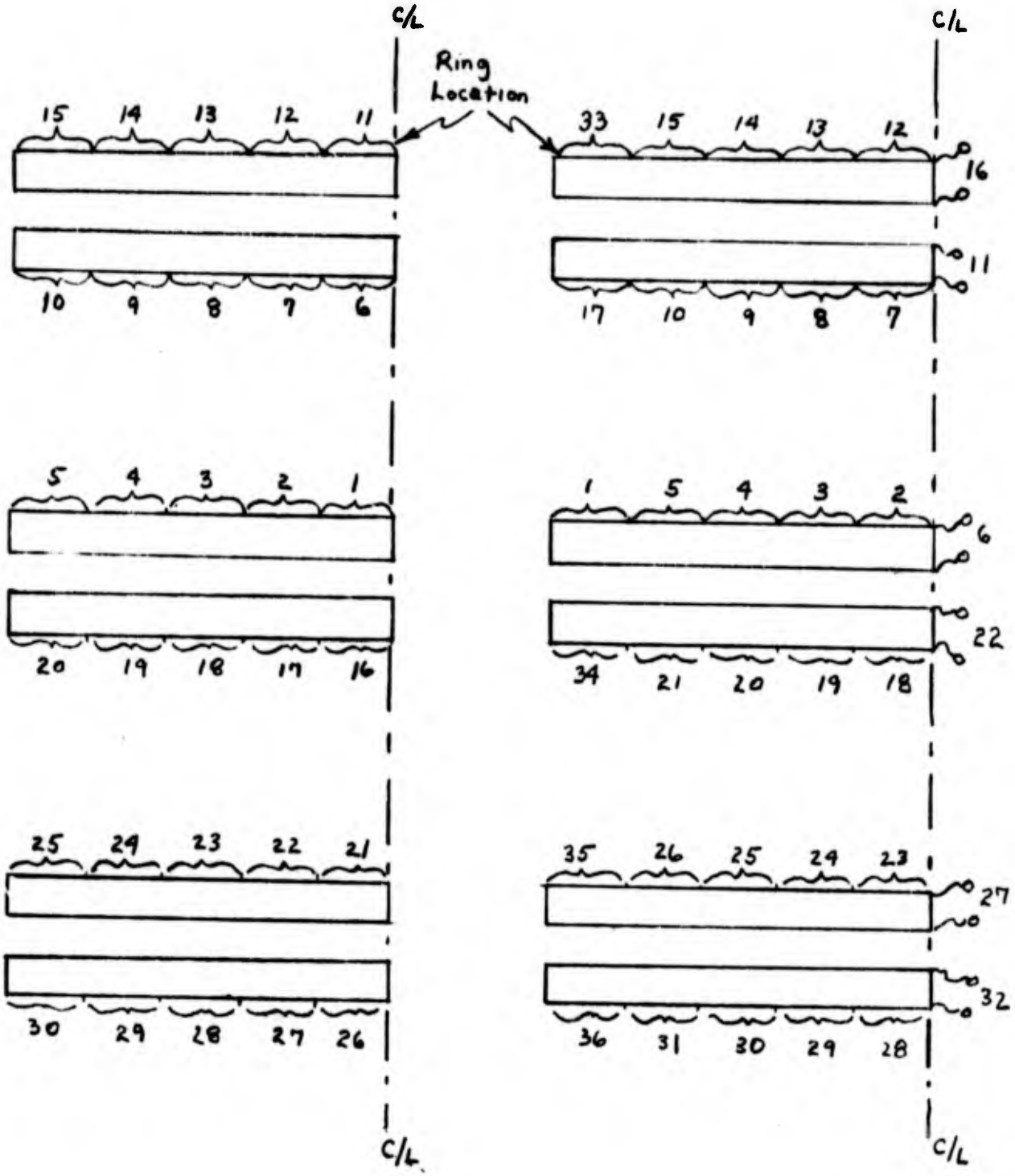

Model for $Z_{i,j}$ Development
(CHIEF Output)

Array Model
(Separate Unloaded and Independent Housings)

Figure B.2 Element Numbering For the Electroacoustic Line Array

One term from the from the above summation can be written as follows:

$$f^*_{k,\ell} = \frac{1}{v_k}\left[\sum_{j}^{\text{ports of disk } \ell}\left\{\sum_{i}^{\text{ports of disk } k} F^*_{i,j}\, V_i\right\}\right] \qquad (3)$$

Since the impedance is defined as the ratio of force to velocity, the equivalent mutual impedance terms of the two port model are defined by equation (4)

$$Z_{k,\ell} = f_{k,\ell} / v_\ell \qquad (4)$$

The multiport forces, $F_{i,j}$, are defined in terms of the multiport $Z_{i,j}$'s by equation (5).

$$F_{i,j} = (R_{i,j} + j\, X_{i,j})\, V_j \qquad (5)$$

Combining equations (3), (4), and (5) results in the following expression for the equivalent two port load impedances:

$$Z_{k,\ell} = \frac{1}{v_\ell\, v^*_k}\left[\sum_{j}^{\text{ports of disk } \ell}\left\{\sum_{i}^{\text{ports of disk } k} (R_{i,j} + j X_{i,j})\, V_j\, V^*_i\right\}\right] \qquad (6)$$

The double summation is the finite element analog of the double integrals by which mutual impedance terms are normally defined.

In numerically evaluating equation (6) a single velocity profile (V) is assumed valid for all disks in the array.

APPENDIX C DYNAMIC PERFORMANCE DATA FOR THE MULTIPORT AND THE TWO PORT MODELS

The tables of this Appendix list the values of average displacement and charge which are direct outputs of the DYANA computer program for the two port models.

To obtain average velocity v or input current i multiply these quantities by $j\omega$.

$$v(1) = 2\pi f \, j \, x(1)$$

$$i(1) = 2\pi f \, j \, q(1)$$

etc.

Because the array was not steered electrically, the three transducers in the lower half array give the same result as those listed for the upper half array. The numbering scheme is as follows:

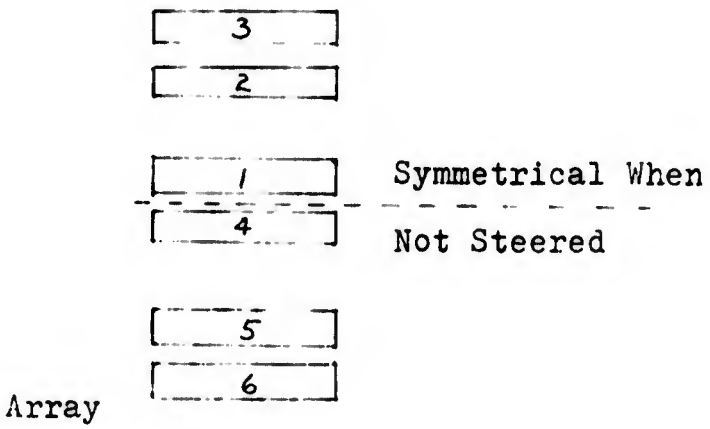

RESULTS OF THE MULTIPORT MODEL

Freq	Parameter	Mag	∠	Mag	∠
	Gap			.050M	
	$\nu(1)$			.2221 10^{-8}	2.9
550.	$\nu(2)$	Not Computed		.2221 "	2.9
	$\nu(3)$			.2842 "	2.4
	$q(1)$			.7156 10^{-7}	-0.2
	$q(2)$			.7156 "	-0.2
	$q(3)$			.6960 "	-0.2
	Gap	.200M		.050M	
	$\nu(1)$	.4111 10^{-8}	1.6	.3994 10^{-8}	1.6
700	$\nu(2)$	.4117 "	1.5	.3994 "	1.6
	$\nu(3)$	.4200 "	1.0	.4181 "	1.3
	$q(1)$	.7759 10^{-7}	-1.0	.8503 10^{-7}	-0.9
	$q(2)$	.7756 "	-1.0	.8502 "	-0.9
	$q(3)$	.7616 "	-0.6	.7637 "	-0.8
	Gap	.200M		.050M	
	$\nu(1)$	1.1142 10^{-8}	-9.5	6.3972 10^{-8}	-111.4
850	$\nu(2)$	1.1117 "	-9.3	6.3944 "	-111.4
	$\nu(3)$	.9575 "	-4.3	.6303 "	23.7
	$q(1)$	1.154 10^{-7}	-7.9	4.703 10^{-7}	-108.9
	$q(2)$	1.151 "	-7.7	4.700 "	-108.9
	$q(3)$	1.026 "	-3.6	.7191 "	17.4
	Gap	.200M		.050M	
	$\nu(1)$	1.171 10^{-8}	-152.9	.3755 10^{-8}	-161.9
1000	$\nu(2)$	1.172 "	-154.1	.3815 "	-162.0
	$\nu(3)$	1.728 "	-165.0	1.695 "	-167.9
	$q(1)$	.1967 10^{-7}	- 75.5	.3160 10^{-7}	- 6.7
	$q(2)$	.1883 "	- 76.1	.3138 "	- 6.9
	$q(3)$	.2396 "	-138.0	.2155 "	-143.7
	Gap	.200M		.050M	
	$\nu(1)$	.3118 10^{-8}	-164.8	.1406 10^{-8}	-168.4
1150	$\nu(2)$	.3115 "	-165.4	.1406 "	-168.4
	$\nu(3)$	.3729 "	-172.9	.3667 "	-173.1
	$q(1)$	.3819 10^{-7}	- 3.9	.4401 10^{-7}	- 1.0
	$q(2)$	.3817 "	- 3.7	.4401 "	- 1.0
	$q(3)$	.3584 "	- 2.3	.3602 "	- 2.2
	Gap	.200M		.050M	
	$\nu(1)$	.1713 10^{-8}	-166.9	.08280 10^{-8}	-169.5
1300	$\nu(2)$	.1707 "	-167.5	.08282 "	-169.5
	$\nu(3)$	.1958 "	-174.2	.1936 "	-174.0
	$q(1)$	.4559 10^{-7}	- 1.3	.4829 10^{-7}	- 0.4
	$q(2)$	.4560 "	- 1.3	.4829 "	- 0.4
	$q(3)$	.4479 "	- 0.7	.4484 "	- 0.7

RESULTS OF THE TWO PORT MODEL DERIVED FROM FREE FIELD LOAD & PROFILE

Freq	Parameter	Mag	∠	Mag	∠
	Gap			.050M	
550	$\nu(1)$	Not Computed		$.2525\ 10^{-8}$	2.
	$\nu(2)$			.2525 "	2.
	$\nu(3)$			.2930 "	1.
	$q(1)$			$.7150\ 10^{-7}$	-0.
	$q(2)$			.7150 "	-0.
	$q(3)$			.6960 "	-0.
	Gap	.200M		.050M	
700	$\nu(1)$	$.4334\ 10^{-8}$	-0.	$.4537\ 10^{-8}$	0.
	$\nu(2)$	.4333 "	-0.	.4537 "	0.
	$\nu(3)$	.4293 "	-0.	.4300 "	-0.
	$q(1)$	$.7753\ 10^{-7}$	-1.	$.8469\ 10^{-7}$	-1.
	$q(2)$	.7749 "	-1.	.8469 "	-1.
	$q(3)$	.7612 "	-1.	.7634 "	-1.
	Gap	.200M		.050M	
850	$\nu(1)$	$1.154\ 10^{-8}$	-12.	$7.040\ 10^{-8}$	-90.
	$\nu(2)$	1.150 "	-11.	7.037 "	-90.
	$\nu(3)$	.9656 "	- 5.	.3494 "	16.
	$q(1)$	$1.143\ 10^{-7}$	- 8.	$4.686\ 10^{-7}$	-86.
	$q(2)$	1.141 "	- 8.	4.684 "	-86.
	$q(3)$	1.023 "	- 3.	.6106 "	6.
	Gap	.200M		.050M	
1000	$\nu(1)$	$1.053\ 10^{-8}$	-155.	$.3729\ 10^{-8}$	-164.
	$\nu(2)$	1.054 "	-156.	.3820 "	-164.
	$\nu(3)$	1.506 "	-166.	1.480 "	-168.
	$q(1)$	$.204510^{-7}$	- 79.	$.3102\ 10^{-7}$	- 8.
	$q(2)$	.1960 "	- 79.	.3065 "	- 8.
	$q(3)$	.2494 "	-139.	.2271 "	-144.
	Gap	.200M		.050M	
1150	$\nu(1)$	$.3297\ 10^{-8}$	-167.	$.1682\ 10^{-8}$	-170.
	$\nu(2)$	.3295 "	-167.	.1682 "	-170.
	$\nu(3)$	.3825 "	-174.	.3783 "	-174.
	$q(1)$	$.3801\ 10^{-7}$	- 4.	$.4374\ 10^{-7}$	- 1.
	$q(2)$	.3799 "	- 4.	.4374 "	- 1.
	$q(3)$	.3573 "	- 2.	.3589 "	- 2.
	Gap	.200M		.050M	
1300	$\nu(1)$	$.1808\ 10^{-8}$	-169.	$.1007\ 10^{-8}$	-171.
	$\nu(2)$	.1804 "	-170.	.1007 "	-171.
	$\nu(3)$	.2004 "	-175.	.1997 "	-175.
	$q(1)$	$.4624\ 10^{-7}$	- 18.	$.5084\ 10^{-7}$	- 20.
	$q(2)$	.4629 "	- 18.	.5084 "	- 20.
	$q(3)$	.4582 "	- 16.	.4581 "	- 16.

RESULTS OF THE TWO PORT MODEL DERIVED FROM ARRAY LOAD DISTRIBUTION FOR SMALL GAP

Freq	Parameter	Mag	∠	Mag	∠
	Gap			.050M	—
550	$\nu(1)$	Not Computed		$.2222\ 10^{-8}$	3.
	$\nu(2)$			.2222 "	3.
	$\nu(3)$			.2739 "	2.
	$q(1)$			$.7156\ 10^{-7}$	-0.
	$q(2)$			.7156 "	-0.
	$q(3)$			.6982	-0.
	Gap	.200M	—	.050M	—
700	$\nu(1)$	$.4092\ 10^{-8}$	1.	$.4019\ 10^{-8}$	1.
	$\nu(2)$	.4092 "	1.	.4019 "	1.
	$\nu(3)$	.4106 "	1.	.4115 "	1.
	$q(1)$	$.7830\ 10^{-7}$	-1.	$.8323\ 10^{-7}$	-1.
	$q(2)$	.7828 "	-1.	.8323 "	-1.
	$q(3)$	.7708 "	-1.	.7651 "	-1.
	Gap	.200M	—	.050M	—
1000	$\nu(1)$	$.7889\ 10^{-8}$	-157.	$.3122\ 10^{-8}$	-164.
	$\nu(2)$	.7889 "	-157.	.3117 "	-164.
	$\nu(3)$	1.018 "	-164.	1.001 "	-165.
	$q(1)$	$.1792\ 10^{-7}$	- 48.	$.3157\ 10^{-7}$	- 6.
	$q(2)$	.1757 "	- 48.	.3158 "	- 6.
	$q(3)$	.1178 "	- 89.	.1080 "	- 86.

RESULTS OF THE TWO PORT MODEL DERIVED BY THE IN AIR PROCEDURE

Freq	Parameter	Mag	∠	Mag	∠
	Gap			.050M	—
550	$\nu(1)$	Not Computed		.4499 10^{-8}	-3.
	$\nu(2)$			.4498 "	-3.
	$\nu(3)$			.3603 "	-2.
	$q(1)$			.7315 10^{-7}	-1.
	$q(2)$			.7315 "	-1.
	$q(3)$			.6959 "	-0.
	Gap	.200M	—	.050M	—
700	$\nu(1)$	.5617 10^{-8}	-6.	.9895 10^{-8}	-10.
	$\nu(2)$	.5601 "	-6.	.9893 "	-10.
	$\nu(3)$	.5080 "	-4.	.5150 "	- 8.
	$q(1)$	.7772 10^{-7}	-2.	.9464 10^{-7}	- 4.
	$q(2)$	.7766 "	-2.	.9463 "	- 4.
	$q(3)$	.7562 "	-1.	.7579 "	- 2.
	Gap	.200M	—	.050M	—
1000	$\nu(1)$	1.477 10^{-8}	-142.	.4242 10^{-8}	-157.
	$\nu(2)$	1.465 "	-144.	.4274 "	-157.
	$\nu(3)$	2.474 "	-157.	2.025 "	-163.
	$q(1)$	.3853 10^{-7}	- 79.	.3969 10^{-7}	- 10.
	$q(2)$	.3616 "	- 80.	.3958 "	- 10.
	$q(3)$	.5535 "	-134.	.3475 "	-134.